Available online at www.sciencedirect.com
SCIENCE DIRECT®
Microelectronic Engineering 77 (2005) 184–192
MICROELECTRONIC ENGINEERING
www.elsevier.com/locate/mee

Interfacial reactions and electrical properties of hafnium-based thin films in Cu/barrier/n^+–p junction diodes

Keng-Liang Ou [a], Ming-Hung Tsai [b], Haw-Ming Huang [a], Shi-Yung Chiou [c], Che-Tong Lin [d], Sheng-Yang Lee [d,e,*]

[a] *Graduate Institute of Oral Sciences, College of Oral Medicine, Taipei Medical University, Taipei 110, Taiwan, ROC*
[b] *Department of Dentistry, En Chu Kong Hospital, Taipei Hsien 237, Taiwan, ROC*
[c] *Department of Mold and Die Engineering, National Kaohsiung University of Applied Sciences, Kaohsiung 807, Taiwan, ROC*
[d] *School of Dentistry, College of Oral Medicine, Taipei Medical University, Taipei 110, Taiwan, ROC*
[e] *Dental Department of Wan-Fang Hospital, Taipei Medical University, Taipei 110, Taiwan, ROC*

Received 2 September 2004; accepted 26 October 2004
Available online 18 November 2004

Abstract

In this study, the barrier properties of Hf and nitrogen incorporated Hf films were investigated by Cu/Hf–N/Si structure. Hafnium and hafnium nitride films were prepared by reactive rf-magnetron sputtering on blank silicon wafers. The barrier properties were evaluated by sheet resistance, X-ray diffraction, transmission electron microscopy, scanning electron microscopy, and X-ray photoelectron spectroscopy. The as-deposited Hf film has a hexagonal close packed structure and a low resistivity of 100.98 μΩ-cm. With increasing nitrogen concentration of Hf–N film, phase transformations are identified as hcp-Hf → fcc-HfN. The thermal stability of Cu/Hf/Si and Cu/$HfN_{0.47}$/Si contact system is evaluated by thermal stressing at various annealing temperatures. Nitrogen incorporated Hf films possess better barrier performance than sputtered Hf films. For the Cu/Hf/Si contact system, the interfacial reaction between the Hf barrier layer and the Cu layer is observed after annealing at 550 °C for 30 min, and copper–hafnium compounds form. Highly resistive copper silicide forms after annealing at 600 °C for 30 min. The Hf barrier fails due to the reaction of Cu and the Hf barrier, in which Cu atoms penetrate into the Si substrate after annealing at high temperature. The Cu/$HfN_{0.47}$/Si is fairly stable up to annealing at 650 °C for 30 min. In addition, no copper–hafnium and copper silicide compounds are found. Diffusion resistance of nitrogen-incorporated Hf barrier is more effective. The thermal stabilities of Cu/$HfN_{0.47}$/n^+–p junction diodes are enhanced by nitrogen incorporation. The Cu/Hf/n^+–p junction diodes result in large reverse-biased junction leakage currents after annealing at 500 °C for 30 min. On the other hand, Nitrogen incorporated Hf diffusion barriers retained the integrity of junction diodes up to 550 °C with lower reverse current densities. Phase transformation of hafnium-based barrier films with nitrogen incorporation are believed to impede Cu diffusion into the Si

* Corresponding author. Tel.: +886 2 27361661x5128; fax: +886 2 27362295.
E-mail address: klou@tmu.edu.tw (S.-Y. Lee).

0167-9317/$ - see front matter
doi:10.1016/j.mee.2004.10.006

substrate and hence improve the barrier performance. Nitrogen incorporated hafnium diffusion barrier can suppress the formation of copper–hafnium compounds and copper penetration, and thus improve the thermal stability of barrier layer.

Keywords: Copper; Hafnium; Nitrides; Sputtering; Junction diodes

1. Introduction

A high performance interconnection network on a chip is becoming increasingly important for ultralarge-scale integration (ULSI) of Si integrated circuits. The use of copper in on-chip metallization of microelectronic devices has recently attracted considerable attention due to its lower electrical resistivity and higher electromigration resistance than aluminum. The use of copper, however, raises several problems. For instance, Cu cannot adhere well to most dielectric substrates and is highly reactive with most metals and semiconductors. Hence, thin film adhesion promoters and diffusion barriers must be used to enhance the adhesion and inhibit diffusion in the Cu-based metallization. Refractory metals have been investigated for metallization applications. Among the barrier films, tantalum-based film has been proven to be one of the most useful barrier materials [1–3]. However, since the resistivities of TaN and Ta–Si–N films are about 200 and 625 μΩ-cm, respectively, these materials are deemed unfavorable for use as low-resistivity diffusion barrier [3–5]. Therefore, new barrier materials with high thermal stability and low electrical resistivity are needed to develop. Other refractory metals probably exhibit very favorable properties, and in particular sputtered hafnium films have been subjected to preliminary evaluation [6–9]. In this article, thermal stability of hafnium-based barrier layers (50 nm) was studied in the Cu metallization system. Furthermore, properties of barrier layers were evaluated by electrical measurements and material analyses.

2. Experimental procedure

The barrier performace of Hf–N films against Cu diffusion was investigated using a structure of Cu/Hf–N/n^+–p junction diodes. The key feature of this experiment is the various nitrogen flow rate during sputtering of Hf–N film formation. First, p-type (1 0 0)-oriented Si wafers with a resistivity 6–9 Ω-cm were used in this study. After standard RCA cleaning, the wafers were administered the LOCOS process to define active regions. The n^+–p junctions were formed by As^+ implantation at 60 keV with a dose of 5×10^{15} cm^{-2} followed by the rapid thermal annealing (RTA) process at 1050 °C for 30 s in N_2 ambient. After the contact windows were cleaned by dipping sample in HF, a reactively sputtered Hf–N film (50 nm) was deposited onto the active regions with various nitrogen flow ratio. In this paper, nitrogen flow ratio is defined as a ratio of N_2 partial flow to total gas flow (N_2 + Ar). Then Cu film with a thickness of 300 nm was deposited subsequently in the same sputtering system without break vacuum. During the sputtering, gas pressure was maintained at 0.8 Pa with a power selected at 500 and 1500 W for Hf–N and Cu, respectively. Finally Cu and Hf–N layers were patterned by dilute HNO_3 and Cl_2 plasma, respectively, for the formation of Cu/Hf–N/n^+–p junction diodes.

To estimate the barrier capability of Hf–N films against Cu diffusion, the devices (Cu/Hf–N/n^+–p junction diode) were thermally annealed at a temperature ranging from 400 to 650 °C for 30 min in a vacuum of 1.33 Pa. For electrical analyses, leakage current of the diodes was measured by HP4145B semiconductor parameter-analyzer at a reverse bias of −5 V. After annealing at various temperatures for 30 min, the diode leakage current was measured. In addition, surface morphologies of the Hf–N films were analyzed by a Nanoscope III atomic force microscope (AFM) with a Si probe. AFM probe was scanned over an area of 5×5 μm^2 with 512 scans at 1 Hz scanning rate in tapping mode. Sheet resistance measurements

were taken using a four-point probe system. Grazing incidence X-ray diffractometry (GIXRD) was used to identify the phases of the films. The compositions of the films were analyzed by X-ray photoemission spectroscopy (XPS) with a monochcrromatic Mg Kα source. The X-ray power was 250W (15 kV at 16.7 mA). The XPS energy scale was calibrated by setting the binding energy of $Ag_{3d5/2}$ line on clean silver to exactly 368.3 eV referenced to the Femi level. The angle of incidence of the X-ray beam with the specimen normal was 45°. High-resolution scans were run for Hf and N using X-ray beam with about a 15 nm diameter. Furthermore, 300 nm thick Cu films were sputtered onto Hf–N films to investigate their ability to resist Cu diffusion. Cu/Hf–N/Si samples were annealed from 450 to 700 °C in vacuum for 30 min to evaluate their barrier stability. Surface morphology of annealed Cu/barrier/Si was observed by scanning electron microscopy (SEM). Compositions of failure sites were analyzed by energy dispersive spectrometry (EDXS) after removing both copper and barrier layers by wet-chemical solution. The interface microstructure was examined by transmission electron microscopy (TEM) and energy dispersive spectrometry (EDXS). Cross-sectional TEM samples were prepared electron transparency by mechanical thinning followed by ion milling in a precision ion polishing system (PIPS).

3. Results and discussion

3.1. Properties of the Hf and Hf–N thin films

Fig. 1 shows a series of X-ray diffraction patterns for different Hf and Hf–N films, deposited on bare silicon substrates under various nitrogen flow rates. The X-ray diffraction pattern of the hafnium film is denoted as (a) in Fig. 1. The (1 0 1) and (1 1 0) peaks confirm that the hafnium films on silicon substrates have a hexagonal close packed structure (α-Hf) (JCPDS 05-0670). The first nitride phase to from is $HfN_{0.4}$ (JCPDS 40-1277) when a small amount of nitrogen is added, as indicated in spectrum (b) of Fig. 1. When the nitrogen content increases to 22.1 at. %, the diffraction pattern of the $HfN_{0.28}$ film contains both narrow and broad peaks, as shown in Fig. 1, denoted as (c). This indicates that at least two phases with different grain sizes are present. It is reported that different phases, α-Hf, ε-Hf_3N_2, ζ-Hf_4N_3, and HfN can exist in a limited composition range [10]. The narrow peaks belong to ε-Hf_3N_2 (JCPDS 24-0466) phase. The broad scanning XRD pattern implies that the $HfN_{0.28}$ film contains some amorphous-like or fine-grained materials. The relatively sharp peaks of the fcc-HfN (JCPDS 33-0592) phase (denoted as (d) in Fig. 1) are observed for the $HfN_{0.47}$ film. The XRD results in Fig. 1 clearly show that α-Hf, $HfN_{0.4}$, ε-Hf_3N_2 and HfN phases form successively as nitrogen flow rate increases from 0 to 3.0 sccm.

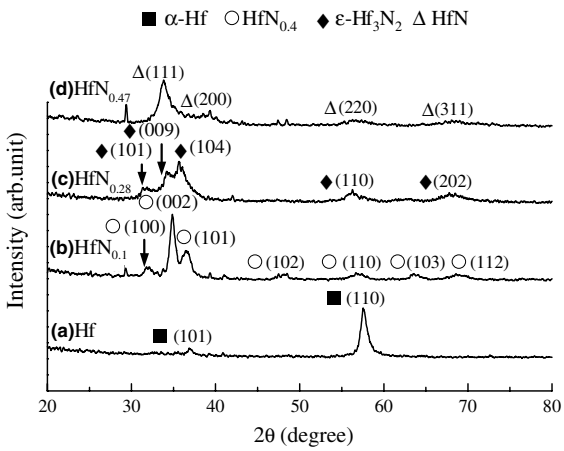

Fig. 1. XRD patterns of the Hf–N films with various nitrogen contents.

To determine the nitrogen concentrations of the Hf–N films deposited at various nitrogen flow rates, chemical compositions are evaluated by XPS. The nitrogen content of the Hf–N film increases with the amount of nitrogen in the sputtering gas. The compositions of Hf–N films deposited at nitrogen flow rates of 1, 2, and 3 sccm, are $HfN_{0.1}$, $HfN_{0.28}$, and $HfN_{0.47}$, respectively. Fig. 2 offers consistent results regarding the critical nitrogen flow rates to form nitrogen-saturated $HfN_{0.1}$ (1 sccm), $HfN_{0.28}$ (2 sccm) and $HfN_{0.47}$ (3 sccm). Fig. 3 also shows the electrical resistivity of Hf–N film as a function of nitrogen flow rate. The

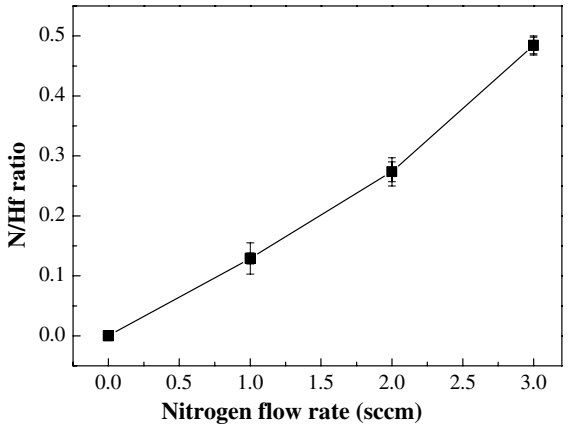

Fig. 2. Composition (N/Hf atomic ratio) plots of Hf-based films deposited on silicon dioxide under various nitrogen flow rates.

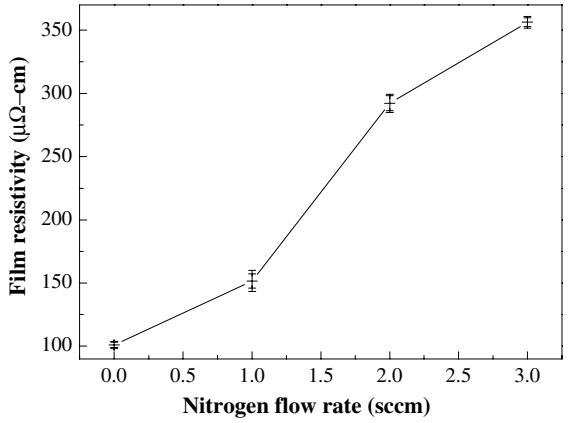

Fig. 3. The electrical resistivity of Hf–N films as a function of nitrogen flow rate.

resistivity of the as-deposited film shows several interesting features. The electrical resistivity of the Hf film is 100.98 μΩ-cm. Resistivity increases slightly when a small amount of nitrogen is added to the sputtering gas. The resistivity of the film increases to 292.17 μΩ-cm when the nitrogen flow rate is 2 sccm. When more nitrogen is incorporated into the Hf film, the resistivity of the $HfN_{0.47}$ film increases to 356.28 μΩ-cm. For comparison, the nitrogen flow rates (1, 2, and 3 sccm) dividing the four regions closely correspond to the flow rates of finding $HfN_{0.4}$, ε-Hf_3N_2, and fcc-HfN from XRD patterns. Moreover, the variations in resistivity are attributed to microstructure and phase transformation.

3.2. Thermal stability of Cu/Hf/Si and Cu/$HfN_{0.47}$/Si systems

Barrier capability of thin Hf and $HfN_{0.47}$ films was investigated by evaluating the thermal stability of Cu/barrier (50 nm)/n^+–p junction diodes using electrical measurements. In this measurement, the reverse current densities were obtained from an average value of 25 samples and the diode area was 1000×1000 μm^2. Fig. 4 illustrates the statistical distributions of reverse bias reverse current density for Cu/barrier (50 nm)/n^+–p junction diodes annealed at various temperatures. For the diodes without annealing, the reverse current densities remain stable (below 10 nA/cm^2) as nitrogen flow ratio is increased. However, the diode leakage increases with increasing the annealing temperature and most diodes are degraded after annealing at 600 °C. As shown in Fig. 4, the reverse current densities initially decrease for 400 °C annealing, and then increase with increasing the annealing temperatures. If a failure criterion is defined as 10^{-6} A/cm^2, the Cu/Hf/n^+–p diodes remained stable after annealing at temperatures up to 450 °C but suffered degradation at 500 °C for 30 min. It is reported that the barrier properties can be improved by adding impurities, such as nitrogen

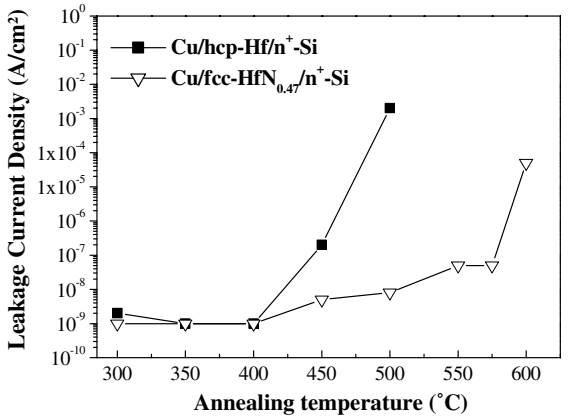

Fig. 4. Variation in reverse current density of Cu/barrier/Si as a function of annealing temperature.

and oxygen [3,13,14,16,17]. It was similar reported results by Tsai et al. It was found that the diodes with 60 nm PVD and CVD metal nitride barriers would begin to deteriorate at 500 and 550 °C for 30 min. [15]. It is shown that barrier capability of Hf–N film is better than that of Hf film without nitrogen incorporation. As nitrogen concentration increases, $HfN_{0.47}$ barrier film was formed. The $Cu/HfN_{0.47}/n^+$–p diodes retained better electrical integrity after annealing at 550 °C with lower reverse current densities. The $HfN_{0.47}$ films have much better barrier performance than Hf barrier film. The improved barrier capability is attributed to finer crystallization and interstitial effect is thought to result in microstructural variation and hence improve barrier capability. It is reported that the microstructure within the barrier layer strongly affects the barrier performance because Cu diffuses through fast diffusion paths such as grain boundaries within the barrier layer [3,15,18].

Fig. 5 plots the GIXRD patterns of the Cu/Hf/Si samples before and after annealing at 550 °C for 30 min. Strong Cu (1 1 1) and weak Cu (2 0 0) peaks are observed in unannealed Cu/Hf/Si sample, implying that the Cu films prefer the (1 1 1) crystal orientation. Copper with a high (1 1 1) texture has been reported to exhibit well resistance to electromigration [11]. The diffraction peaks of α-Hf (1 0 1) and Cu (1 1 1) clearly disappear and the $CuHf_2$ phase appears for Cu/Hf/Si sample annealed at 550 °C for 30 min. These results show that the interdiffusion of Cu and Hf induces the formation of Cu–Hf and Cu–Hf–Si compounds. Fig. 6 shows XRD patterns of the Cu/Hf/Si and $Cu/HfN_{0.47}/Si$ samples after annealing at 600 °C for 30 min. Strong Cu_3Si peaks are observed for annealed Cu/Hf/Si sample. It reveals that high-resistance copper silicide compounds were formed after 600 °C annealing. It also indicates the degradation of the Hf barrier after annealing. The as-deposited Hf film consists of fine columnar grains. The degradation of the Hf barrier is attributed to the diffusion of Cu into the Si substrate through the columnar Hf barrier. Strong Cu (1 1 1), weak Cu (2 0 0), and HfN (1 1 1) peaks are found in the XRD spectrum of annealed $Cu/HfN_{0.47}/Si$ sample. The intensity of the HfN peak is lower. That is, it has a higher full width at half maximum (FWHM). The as-deposited $HfN_{0.47}$ barrier film has an amorphous-like structure [12]. Neither Cu–Si nor Cu–Hf and Cu–Hf–Si compounds are observed after annealing at 600 °C for 30 min. The results reveal that the $HfN_{0.47}$ barrier is more effective in preventing Cu diffusion than the Hf barrier film. The Cu–Hf and Cu–Hf–Si compounds are not observed in $Cu/HfN_{0.47}/Si$ sample after annealing. The diffraction peaks of HfN phases are observed. These results show that nitrogen incorporation in the Hf film can suppress the formation of Cu–Hf(–Si) compound. Fig. 7 shows XRD patterns of the $Cu/HfN_{0.47}/Si$ samples after annealing at 650 °C and 700 °C for 30 min. The

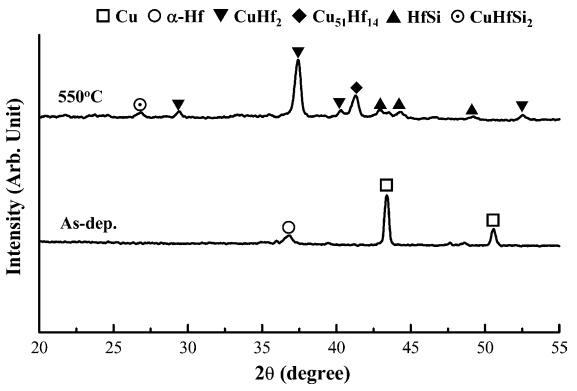

Fig. 5. XRD patterns of Cu/Hf/Si systems before and after annealing at 550 °C for 30 min.

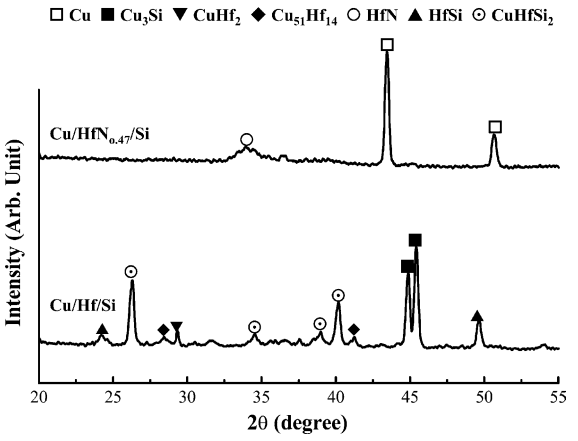

Fig. 6. XRD patterns of of Cu/Hf/Si and $Cu/HfN_{0.47}/Si$ systems after annealing at 600 °C for 30 min.

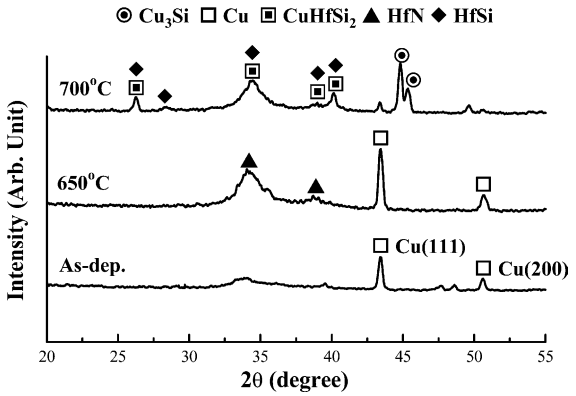

Fig. 7. XRD patterns of Cu/$HfN_{0.47}$/Si contact systems before and after annealing at 650 and 700 °C for 30 min.

intensity of the HfN (1 1 1) peak increases obviously after 650 °C-annealing. This result reveals that annealing causes development of HfN crystals. Copper silicide phases are found obviously for Cu/$HfN_{0.47}$/Si samples annealed at 700 °C for 30 min.

Fig. 8 shows the SEM-EDXS and cross-sectional TEM micrographs of Cu/Hf/Si after annealing over the failure temperature. As shown in Fig. 8(a), protrusions were observed on the surface, indicating a severe reaction of Cu/Hf/Si. Fig. 8(a) shows EDXS spectrum of the protrusion (denoted as A). It revealed that the protrusion consisted of copper and silicon element and was a copper rich region. These protrusions were presumably caused by Cu diffusion through the localized weak points in the barrier and reacting with underlying Si to form Cu_3Si. Similar phenomena were observed for Ta diffusion barriers by Wu et al. [18]. Fig. 8(b) and Fig. 9 are shown the local phase determination by analytical methods of cross-sectional TEM and EDXS. Fig. 8(b) shows the cross-sectional TEM image of Cu/Hf/Si sample after annealing at 600 °C for 30 min. It is obvious that hafnium silicide and copper silicide were observed after annealing, and the interface of the sample was not clear. It indicates the degradation of the Hf barrier after annealing at 600 °C for 30 min. The as-deposited Hf film consists of fine columnar grains. The degradation of the Hf barrier is attributed to the diffusion of Cu into the Si substrate through the columnar Hf barrier. Trapezoidal

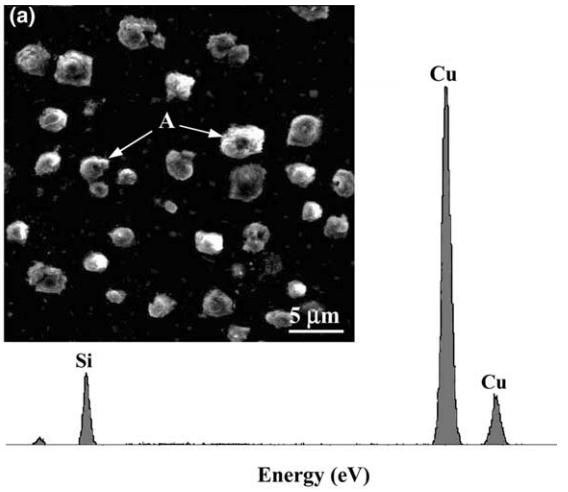

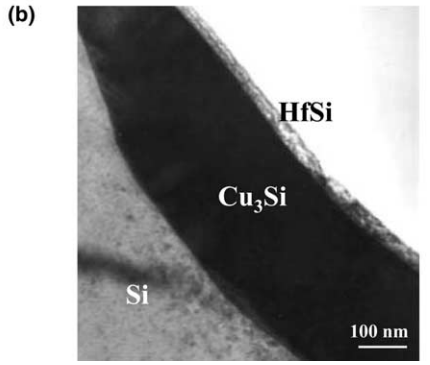

Fig. 8. (a) SEM micrograph and EDS spectrum obtained from the precipitate of Cu/Hf/Si sample annealed at failure temperature, and (b) cross-sectional TEM micrograph of Cu/Hf/Si annealed at 550 °C for 30 min.

copper silicide spikes bounded by Si {1 1 1} and Si {001} planes were observed [13]. Fig. 9 shows cross-sectional TEM micrograph of Cu/$HfN_{0.47}$/Si systems after annealing at various temperatures. Fig. 9(a) shows the TEM image of the Cu/$HfN_{0.47}$/Si sample after annealing at 650 °C for 30 min. The multilayered structure is obvious. No copper silicides are observed at the interface, demonstrating the excellent barrier properties. Fig. 9(b) shows cross-sectional TEM micrograph of 700 °C-annealed Cu/$HfN_{0.47}$/Si. Trapezoidal copper silicide compound is observed, demonstrating the Cu diffusion into Si substrate. These investigations of TEM are in agreement with the XRD results, which indicate the diffusion of Cu atoms through

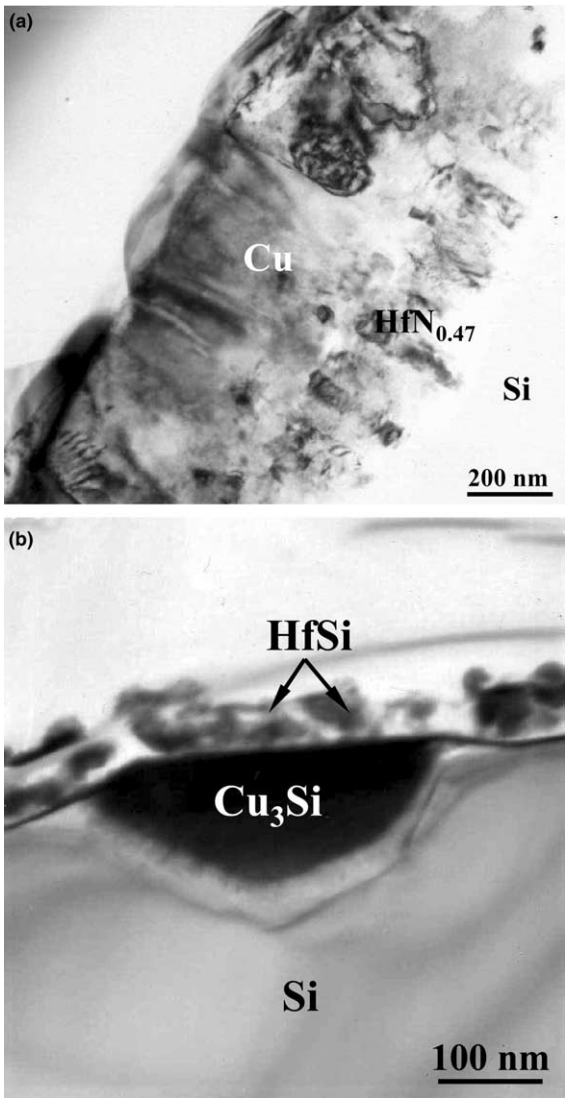

Fig. 9. The cross-sectional TEM micrograph of Cu/$HfN_{0.47}$/Si annealed at: (a) 650 °C, and (b) 700 °C for 30 min.

$HfN_{0.47}$ layer and the formation of compounds containing Cu, Hf and Si are the main causes of failure for Cu/$HfN_{0.47}$/Si barrier layer.

3.3. Failure mechanism of Cu/hcp-Hf/Si and Cu/fcc-HfN/Si system

The GIXRD patterns, SEM-EDS, XTEM and reverse current density clearly reveal a difference between the failures of hafnium and hafnium nitride barriers. Nitrogen incorporated hafnium film has improving barrier capability against copper diffusion. Nitrogen is incorporated into the hafnium and it induces phase transformation to hafnium nitride. The interstitial effect is thought to induce microstructural variation and thereby improve barrier performance. Fig. 10 schematically reveals cross-sections of the interfacial structures of the Cu/Hf/Si and Cu/$HfN_{0.47}$/Si systems before and after annealing. Cu films on Hf–N barriers have a preferred {1 1 1} orientation. The as-deposited Hf barrier has an hcp-Hf structure with columnar grains. The formation of $CuHf_2$ and hafnium silicide is observed after annealing at 550 °C for 30 min, revealing barrier degradation. The mechanism by which the barrier fails involves the sacrificial reaction of Hf with Cu and the motion of Cu through columnar Hf barrier to form Cu_3Si. The barrier capability of Hf film against Cu diffusion can be improved by incorporating nitrogen into Hf films using reactive sputtering. Adding impurities, such as nitrogen and oxygen has been reported to improve the barrier properties of refractory metals [3,13,14]. The as-deposited $HfN_{0.47}$ barrier has the fine-grained fcc-HfN

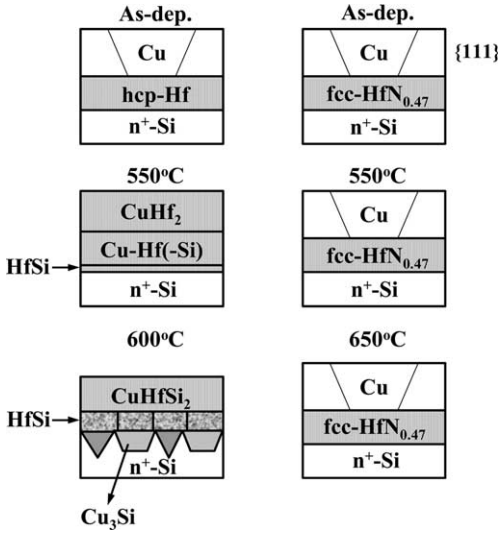

Fig. 10. Schematic illustrations of the microstructures of: (a) Cu/Hf/Si, (b) Cu/$HfN_{0.1}$/Si, (c) Cu/$HfN_{0.28}$/Si, and (d) Cu/$HfN_{0.47}$/Si contact systems before and after annealing.

phases. Neither Cu–Si nor Cu–Hf(–Si) compounds are observed for the Cu/$HfN_{0.47}$/Si sample annealed at 550 °C for 30 min, revealing better barrier performance than hafnium barrier. However, enhancing crystalline structure of the $HfN_{0.47}$ barrier is found after annealing at 600 °C for 30 min. Cu_3Si compounds are not observed for the Cu/$HfN_{0.47}$/Si contact system annealed at 650 °C. The microstructural transition of nitrogen-incorporated hafnium film alleviates the copper diffusion and, therefore, enhances the stability of the barrier and restrains the formation of copper–hafnium compounds. Cu/Hf–N/Si contact system with high thermal stability is obtained.

4. Conclusion

Microstructure variations of hafnium barrier film with various nitrogen concentrations were investigated by Hf/Si and Hf–N/Si. Furthermore, barrier performances against Cu diffusion were evaluated for Cu/Hf/Si and Cu/Hf–N/Si contact systems. A thermally stable Cu/Si contact system, with a low resistivity Hf–N diffusion barrier, is successfully demonstrated. The as-deposited Hf film has a hexagonal close packed structure and a low resistivity of 100.98 μcm. Phase transformations are identified as α-Hf $\rightarrow$ $HfN_{0.4}$ $\rightarrow$ ε-Hf_3N_2 $\rightarrow$ fcc-HfN with increasing nitrogen concentration of Hf–N film. Cu_3Si compounds are found for Cu/Hf/Si contact systems after annealing at 600 °C for 30 min. The mechanism by which the Hf barrier fails involves the sacrificial reaction of Hf with Cu and the motion of Cu through columnar Hf barrier to form Cu_3Si. The Cu/$HfN_{0.47}$/Si contact system tolerates annealing at 650 °C for 30 min without any reaction. Cu_3Si compounds are observed after annealing at 700 °C due to accelerating Cu diffusion through crystalline Hf–N barrier. The thermal stabilities of Cu/$HfN_{0.47}$/n^+–p junction diodes are enhanced by nitrogen incorporation. The Cu/Hf/n^+–p junction diodes result in large reverse-biased junction leakage currents after annealing at 500 °C for 30 min. $HfN_{0.47}$ barrier retained the integrity of junction diodes up to 550 °C with low reverse current densities. Phase transformation of hafnium-based barrier films with nitrogen incorporation are believed to impede Cu diffusion into the Si substrate and hence improve the barrier performance. Nitrogen incorporated hafnium diffusion barrier can suppress the formation of copper–hafnium compounds and copper penetration, and thus improve the thermal stability of barrier layer.

Acknowledgements

The work was financially supported by the National Science Council of the Republic of China under Contract No. NSC92-2314-B-038-012 and this study was sponsored by the Taipei Medical University (TMU92-AE1-B02).

References

[1] D.S. Yoon, H.K. Baik, S.M. Lee, J. Vac. Sci. Technol. B 17 (1) (1999) 174–181.
[2] H. Ono, T. Nakano, T. Ohta, Appl. Phys. Lett. 64 (12) (1994) 1511–1513.
[3] C.E. Ramberg, E. Blanquet, M. Pons, C. Bernard, R. Madar, Microelectron. Eng. 50 (2000) 357–368.
[4] E. Kolawa, J.S. Chen, J.S. Reid, P.J. Pokela, M.A. Nicolet, J. Appl. Phys. 70 (1991) 1369–1373.
[5] J.O. Olowolafe, I. Rau, K.M. Unruh, C.P. Swann, Z.S. Jawad, T. Alford, Thin Solid Films 365 (2000) 19–21.
[6] I. Suni, M. Mäenpää, M.A. Nicolet, M. Luomajärvi, J. Electrochem. Soc. 130 (1983) 1215–1218.
[7] S. Shinkai, K. Sasaki, Jpn. J. Appl. Phys. 38 (1999) 3646–3650.
[8] B.O. Johansson, J.E. Sundgren, U. Helmersson, J. Appl. Phys. 58 (8) (1985) 3112–3117.
[9] S. Shinki, K. Sasaki, Jpn. J. Appl. Phys. 38 (1999) 2097–2102.
[10] B.O. Johansson, J.E. Sundgren, U. Helmersson, M.K. Hibbs, Appl. Phys. Lett. 44 (7) (1984) 670–672.
[11] D. Save, F. Braud, J. Torres, F. Binder, C. Müller, J.O. Weidner, W. Hasseand, Microelectron. Eng. 33 (1997) 75–84.
[12] S.Y. Chiou, K.L. Ou, W.F. Wu, C.P. Chou, Y.M. Chang. Effect of nitrogen addition on microstructure and thermal stability of hafnium nitride diffusion barriers in copper metallization, in: Proceedings of Symposium on Nano Device Technology, 2002, p. 65.
[13] K. Holloway, P.M. Fryer, C. Cabral Jr., J.M.E. Harper, P.J. Bailey, K.H. Kelleher, J. Appl. Phys. 71 (11) (1992) 5433–5444.
[14] X. Sun, E. Kolawa, J.S. Chen, J.S. Reid, M.A. Nicolet, Thin Solid Films 236 (1993) 347–351.

[15] M.H. Tsai, S.C. Sun, C.E. Tsai, S.H. Chuang, H.T. Chiu, J. Appl. Phys. 79 (9) (1996) 6932–6938.
[16] K.H. Min, K.C. Chun, K.B. Kim, J. Vac. Sci. Technol. B 14 (5) (1996) 3263–3269.
[17] G.S. Chen, S.T. Chen, J. Appl. Phys. 87 (12) (2000) 8473–8482.
[18] W.F. Wu, K.L. Ou, C.P. Chou, C.C. Wu, J. Electrochem. Soc. 150 (2) (2003) G83.